

## Excitons and polaritons in ZnSe

Bernard Sermage

*Centre National d'Etudes des Télécommunications, \* 196, rue de Paris, 92220 Bagneux, France*

Guy Fishman

*Groupe de Physique des Solides de l'Ecole Normale Supérieure, \* Université Paris VII, 2, Place Jussieu, 75221 Paris Cedex 05, France*

(Received 24 November 1980)

We have performed resonant Brillouin scattering experiments in ZnSe in the [100] and [110] directions. These two directions are needed to obtain the exciton-polariton dispersion curves without ambiguity. Even if only the influence of the isotropic part of the exchange interaction on heavy and light excitons is taken into account, the number of polariton branches is shown to be dependent on the wave-vector direction. However, in ZnSe a three-branch-polariton model ("quasi-isotropic" model) is enough to account for the experimental results. We obtain thus the longitudinal-transverse (triplet) splitting  $E_{LT} = 1.45 \pm 0.05$  meV, and the quintuplet-transverse (triplet) splitting  $\delta = -0.1 \pm 0.1$  meV, and the masses of heavy and light excitons,  $M_h$  and  $M_l$ ,  $M_h(100) = 1.11 \pm 0.1m_0$ ,  $M_l(100) = 0.3 \pm 0.05m_0$ ,  $M_h(110) = 1.95 \pm 0.1m_0$ ,  $M_l(110) = 0.37 \pm 0.05m_0$  in the free-electron mass unit. These numerical values are little altered if the linear  $k$  term is taken into account.

### I. INTRODUCTION

The problem of the calculation of the exciton dispersion curve in semiconductors with a degenerate valence band has been cleared up in both indirect and direct gap semiconductors by Kane.<sup>1</sup> Contrary to the case of a nondegenerate band<sup>2</sup> this problem has no analytical solution and at first sight the theory is not expected to be as precise as in the case of a nondegenerate band. From an experimental point of view this theory was first checked in an indirect-gap semiconductor (germanium).<sup>3</sup> In direct-gap semiconductors, with which we are dealing in the following, the light alters the exciton dispersion curve and leads to the so-called polariton.<sup>4,5</sup> To obtain the polariton, dispersion curve it is well known that a resonant Brillouin scattering<sup>6</sup> experiment is a well suited tool [GaAs (Ref. 7), CdS (Ref. 8), CdSe (Ref. 9)] although it is not the only one [CuCl (Ref. 10), CuBr (Ref. 11)]. In the case of a degenerate valence band, a simple model leads to a three-branch-polariton dispersion curve.<sup>12</sup> The choice of a "good" semiconductor to test this model is very restricted. In III-V semiconductors the exchange interaction is too small and in I-VII semiconductors the effect linked to a degenerate valence band can be hidden by the linear  $k$  term.<sup>11</sup> Thus it is easy to predict that a "good" semiconductor belongs to II-VI compounds.<sup>13</sup> Among the cubic II-VI semiconductors Zn compounds have the greatest exchange interaction and indeed the choice of ZnSe was guided by the availability of very good samples.<sup>14</sup> A complete calculation of exciton and polariton dispersion curves near the Brillouin-zone center taking into account the linear  $k$  term, the iso-

tropic and the anisotropic part of the exchange interaction, is reported in Ref. 11. In the case of ZnSe, we shall see that the isotropic part of the exchange interaction is sufficient to explain the experimental results. Even in this case the number of exciton branches coupled to light and therefore the number of polariton branches depends on the wave-vector direction. This result can be deduced from group theory<sup>11</sup> but we have taken another point of view and we have written explicitly the exciton wave functions.

In Ref. 1, the exciton wave function is expanded in the eight-dimensional space of the  $n=1$  exciton ground state; the periodic part of the wave functions belongs to the  $\Gamma_6 \times \Gamma_8$  representation which describes the conduction and the degenerate valence band of direct-gap semiconductors such as ZnSe. Taking an intuitive point of view, we recall in the following (Sec. III A) the part of this theory which is useful to study polariton dispersion. A more complete treatment leading to the dispersion of the exciton states  $n=1, 2, \dots$  has been done by Altarelli and Lipari.<sup>15</sup> Contrary to the theory of Kane<sup>1</sup> which is based on a perturbation calculation, Altarelli and Lipari<sup>15</sup> used a variational method and developed the exciton wave function in a larger dimension space than in Ref. 1 so that the accuracy must be better. In this paper we shall content ourselves with the eight-dimensional space of the exciton ground state. We must note that the theories of Refs. 1 and 15 lead to the same number of exciton branches near the center of the Brillouin zone and more precisely to two kinds of excitons: heavy and light ones.

In those theories the linear  $k$  term<sup>16</sup> is not considered. This term splits the valence band into two,

three, and four branches in the [100], [111], and [110] directions, respectively, and thus can induce further splittings in the [111] and [110] directions but not in the [100] direction. As was said above, this term is needed in CuBr but there is not clear evidence that such is the case for ZnSe. Nevertheless, we have taken it into account and a discussion of its relevancy is given at the end of the theoretical part.

The outline of this paper is as follows: In Sec. II we present our experimental results and the numerical values of the parameters which give the best fit within a simple model detailed in Sec. III. In Sec. IIIA we give the wave functions needed for the calculation of polariton effect and we recall the eigenvalues. In Sec. IIIB we give precisely the exact form of the exchange interaction used here. In Sec. IIIC we give the theoretical dispersion curve in the [100] and [110] directions. This permits us to justify the model used to interpret the experimental results. The linear  $k$  term is included in Sec. IIID and is used for the discussion given in Sec. IV. We present our conclusions in Sec. V.

## II. EXPERIMENT

### A. Principle

The resonant Brillouin scattering experiment is now a classical one and has been described in many papers<sup>7,14</sup> (Fig. 1). We work in a backscattering geometry, that is to say that the incident beam and the direction of observation are perpendicular to the surface of the ZnSe sample. The incident beam is produced by a dye laser working with Styloben 3 pumped by the uv lines of an argon laser. The spectral resolution of the dye laser is obtained with a triple Lyot filter and a 1-mm-thick glass plate used as Fabry-Perot. To analyze the scattered light, we use a simple monochromator with a focal length of 1.5 m so that the total resolution is better than 0.03 meV. For practical considerations, the incident and observation directions make an angle of 12°. The aperture of the lens situated between the sample and the monochromator is  $f/6$ . Because of the in-

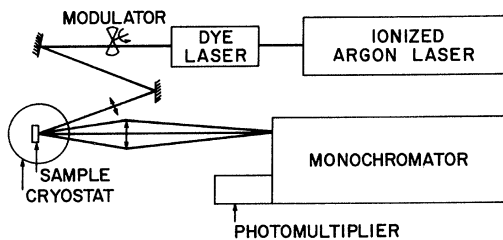


FIG. 1. Experimental setup.

dex of ZnSe which is about 3, the light beams inside the sample are not misoriented by more than 4° relative to the normal to the sample surface. The sample is in the vacuum and cooled by a contact with the cold finger of a helium cryostat so that its temperature is about 10 K.

Brillouin scattering is the scattering of light by the acoustical phonons. The elementary processes are creation or absorption of a phonon. The energy  $E_s$  and the wave vector  $\vec{K}_s$  of the two scattered waves are given by the conservation relations

$$E_s = E_i \pm \Omega, \quad (1)$$

$$\vec{K}_s = \vec{K}_i + \vec{q}, \quad (2)$$

where  $E_i$  and  $\vec{K}_i$  are the energy and the wave vector of the incident light inside the sample and  $\Omega$  and  $\vec{q}$  are the energy and the wave vector of the acoustical phonon.

In the range of wave vectors  $\vec{q}$  of interest ( $q \leq 8 \times 10^6 \text{ cm}^{-1}$ ), which can be of the order of 15% of the Brillouin zone ( $5.5 \times 10^7 \text{ cm}^{-1}$ ), the energy of the acoustical phonons is given by the linear relation

$$\Omega = \hbar v_s q, \quad (3)$$

where  $v_s$  is the sound velocity.

Far from resonance, the light dispersion is linear and the Brillouin shift  $\Delta E$  is the same for the Stokes and the anti-Stokes scattering and is given by

$$\Delta E = |E_s - E_i| = 2 \frac{v_s n}{c} E_i, \quad (4)$$

where  $n$  is the optical index and  $c$  is the light velocity. Near resonance, incident radiation propagates in the sample in a polariton mode, the dispersion of which is generally given by an implicit equation

$$F(E, K) = 0. \quad (5)$$

In the case of ZnSe, this equation has three solutions, as we will see in Sec. III, corresponding to the three polariton branches<sup>14</sup> (Fig. 2)

$$E_j = f_j(K), \quad j = 1, 2, 3. \quad (6)$$

These functions  $f_j$  can be inverted as follows:

$$K_j = f_j^{-1}(E). \quad (7)$$

The Stokes and anti-Stokes shift corresponding to transitions between the branch  $j$  and the branch  $l$  are given by the following equations:

$$\begin{aligned} \Delta E(S_{jl}) &= |E(S_{jl}) - E_i| \\ &= \hbar v_s [f_l^{-1}(E_i - \Delta E(S_{jl})) + f_j^{-1}(E_i)], \end{aligned} \quad (8)$$

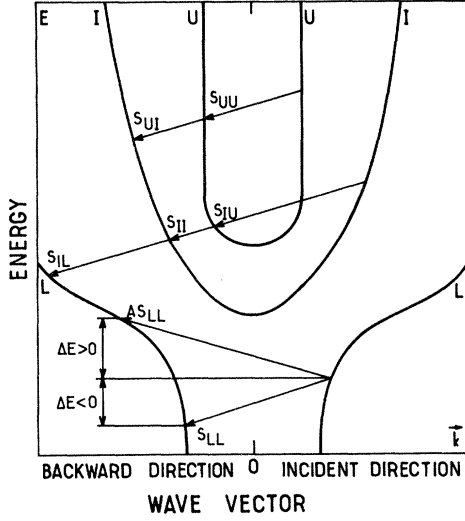


FIG. 2. Sketch of the three-branch polariton. The index of the branches are  $U$ : uppermost,  $I$ : intermediate,  $L$ : lowest branch.  $S_{ij}$  ( $AS_{ij}$ ) ( $i, j = U, I, L$ ) corresponds to a Stokes (anti-Stokes) transition from the branch  $i$  to the branch  $j$ . Some transitions are explicit.  $\Delta E$  is the negative (positive) Stokes (anti-Stokes) shift which is experimentally measured.

$$\Delta E(AS_{ij}) = |E(AS_{ij}) - E_i| = \hbar v_s [f_i^{-1}(E_i + \Delta E(AS_{ij})) + f_j^{-1}(E_i)]. \quad (9)$$

### B. Results

We have performed resonant Brillouin scattering experiments in the [100] and [110] directions and we have used the three-branch-polariton model<sup>12</sup> whose sketch is given in Fig. 2 to identify the peaks. Some examples of the Brillouin spectra in the [100] direction are given in Fig. 3. For energies below that of the resonance, we observe one Stokes and one anti-Stokes Brillouin peak which correspond to an interaction with the longitudinal-acoustic phonons. We have measured the light refractive index at 4.462 Å and we find  $n = 2.86 \pm 0.05$ . We can thus calculate from Eq. (4) the velocities of sound which are given in

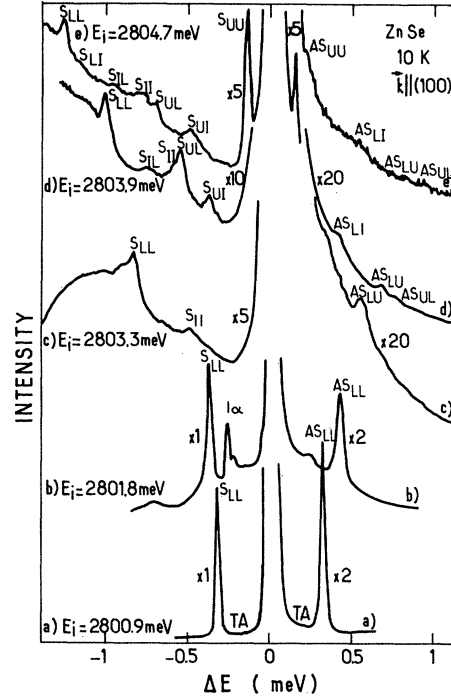


FIG. 3. Brillouin spectra obtained in the [100] direction for different incident energies. The small peaks TA correspond to interaction with transverse-acoustic phonons: This interaction, forbidden from symmetry considerations, is slightly allowed because incident and scattered light are not strictly parallel.

Table I. Our values compare well with the one we can calculate from the elastic constants measured at low temperature by Lee.<sup>17</sup> Near the resonance we observe one or two small peaks which correspond to the interaction with the transverse-acoustic phonons. The velocities of these transverse vibrations are also given in Table I.

We have plotted the shift of the Brillouin peaks as a function of the incident energy in the [100] and [110] direction (Figs. 4 and 5). The identification of the points needs to fit with a theoretical model. At this point we want to make some re-

TABLE I. Velocity of sound in ZnSe. The experiments were performed at 2778 meV, i.e., 24 meV below the resonance. Owing to the slight angle between incident and scattered light, the transverse phonons are observed in the [100] experimental configuration.

Direction	Sound velocity(km/s)			
	LA phonon		TA phonon	
	Our experiment	Reference 17	Our experiment	Reference 17
[100]	4.21 ± 0.15	4.11	2.67 ± 0.10	2.80
[110]	4.82 ± 0.15	4.62	2.82 ± 0.10	2.80
			2.05 ± 0.10	1.86
[111]	4.93 ± 0.15	4.77	2.35 ± 0.10	2.22

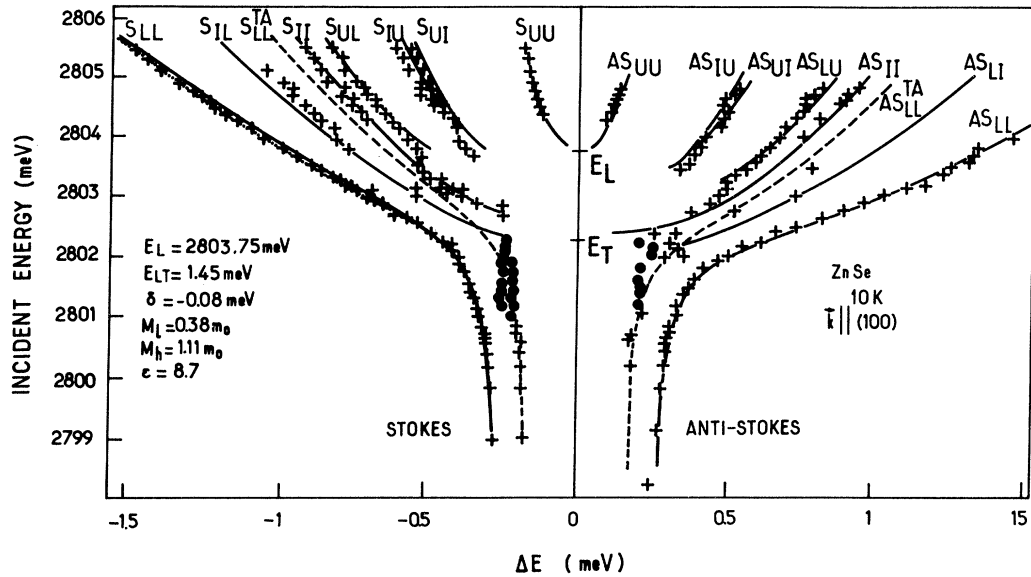


FIG. 4. Stokes ( $\Delta E < 0$ ) and anti-Stokes ( $\Delta E > 0$ ) Brillouin shift versus the incident energy in the [100] direction. Crosses (+) correspond to experimental points of Brillouin scattering and solid circles (●) are attributed to excited states of  $I_2$ . Numerical values quoted in this figure as the solid and dashed lines (LA and TA phonon) are calculated without the linear  $k$  term. Dotted line (LA phonon) is calculated taking into account the linear  $k$  term using the following values:  $\delta = -0.09$  meV,  $M_l = 0.41m_0$ ,  $M_h = 1.04m_0$  linear  $k$  term  $C = 3.3 \times 10^{-10}$  eV cm; other parameters are unchanged.

marks.

(a) The shift with respect to incident frequency is constant (0.23 meV) for some lines (hereafter denoted  $I_\alpha$ ) for an incident energy range between

2801 and 2802 meV. The  $I_\alpha$  peaks are noted by a circle in Figs. 4 and 5. Moreover, this shift does not depend on the direction [100] or [110], whereas the Brillouin shift of all other points

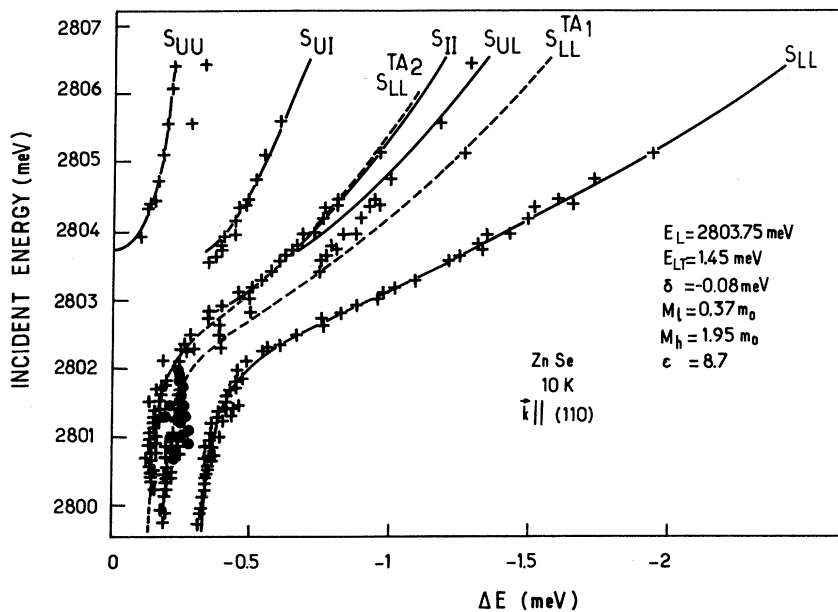


FIG. 5. Stokes Brillouin shift versus the incident energy in the [110] direction. Crosses (+) and solid circles (●) have the same meaning as in Fig. 4. Solid lines (LA phonon) and dashed lines (TA phonon) are calculated with the numerical values quoted here. The sound velocities are given in Table I.

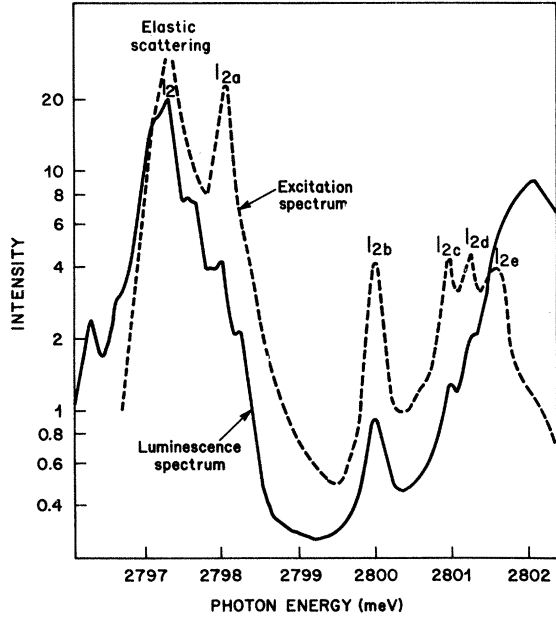


FIG. 6. Solid lines: luminescence spectrum (with an excitation energy above the band gap). Dashed line: excitation spectrum of  $I_2$  showing five excited states of  $I_2$  noted  $I_{2\alpha}$  ( $\alpha = a, b, c, d, e$ ). The three last are situated between 2801 and 2802 meV.

varies with the direction because of the variation of the sound velocity. We thus think that the  $I_\alpha$  peaks do not correspond to Brillouin scattering on excitonic polaritons. Furthermore, in the energy 2801–2802 meV there are three excited states ( $I_{2c}, I_{2d}, I_{2e}$  in Fig. 6) of  $I_2$  which are split by 0.23 meV on both the excitation spectrum and luminescence spectrum of  $I_2$ . The  $I_\alpha$  peaks have an intensity which is maximum for an energy equal to that of  $I_{2e}$ . Now we think that the  $I_\alpha$  peaks observed on the Brillouin spectrum correspond to transitions between two excited states of  $I_2$ , as already observed in Ref. 9. Let us note that the shift of the  $I_\alpha$  peaks is close to (i) the shift of TA-phonon scatterings in the [100] direction, which are not strictly forbidden due to the slight angle between incident and scattering light and (ii) the shift of possible scattering of an intermediate branch in a former interpretation.<sup>14</sup> We must note that our new interpretation of peaks  $I_\alpha$  does not qualitatively change the contents of Ref. 14 but alters quantitatively the parameters in a significant way. The fit we finally obtain is given in Figs. 4 and 5 and its accuracy is discussed in the following sections.

(b) We have tried to fit the experimental points in a classical model of a two-branch polariton valid in the case of a nondegenerate valence band. This model agrees with the points  $S_{UV}$  and  $S_{LL}$

(see Fig. 7). However, it is worth noting that a number of experimental points which are well accounted for in the three-branch-polariton model should *not* exist in the two-branch model.

From another point of view, Fig. 5 shows it is difficult in the [110] direction to discriminate between Stokes scattering inside the lowest branch by transverse phonons and scattering inside the intermediate branch by longitudinal phonons, contrary to the case of the [100] direction. All this shows that experiments in several directions allow us to obtain without ambiguity the three-branch-polariton dispersion curve in ZnSe. Our numerical results are summarized in Table II.<sup>22</sup>

### III. THEORY

#### A. Eigenfunctions and eigenvalues of the exciton Hamiltonian

The Hamiltonian leading to exciton states can be written as<sup>1</sup>

$$H_K = H_c + H_v - e^2/\epsilon r, \quad (10)$$

where  $H_c$  and  $H_v$  are the Hamiltonian describing the conduction and the valence band and  $-e^2/\epsilon r$  is the effective Coulomb interaction,  $\epsilon$  being the dielectric constant and  $r$  the distance between the electron and the hole.

Following Ref. 1, in a direct-gap semiconductor, the so-called relative momentum induces a term proportional to a four-dimensional identity, and an average mass  $M_a$  [defined in Eq. (17) below] results from this. This relative momentum does not lead to any splitting and cannot alter the eigenfunctions. The whole calculation leads to splitting which is *identical* to Eq. (15) below; the Hamiltonian giving this splitting has the symmetry of the Luttinger Hamiltonian.<sup>23</sup> Because we need exciton wave functions to compute the polariton dispersion curve we wish here to show what can be deduced from a simple examination of  $H_K$ .

The eigen-wave-functions of  $H_c$  are  $|S\uparrow\rangle$  and  $|S\downarrow\rangle$ , the quantization axis being arbitrary.  $S$  is a  $\Gamma_1$ -type wave function and  $\uparrow$  or  $\downarrow$  stand for spin up or down. These functions will be written  $|\sigma\rangle$  ( $\sigma = \uparrow$  or  $\downarrow$ ) in the following.

The Hamiltonian  $H_v$  is the Luttinger Hamiltonian<sup>23</sup> (at zero magnetic field) and the eigen wave functions are of  $\Gamma_8$  symmetry. Let us take the quantization axis parallel to the hole wave vector. A simple basis is given by  $|\frac{3}{2}, m\rangle$  ( $m = -\frac{3}{2}, -\frac{1}{2}, \frac{1}{2}, \frac{3}{2}$ ) which we write merely  $|m\rangle$  below. The Hamiltonian  $H_v$  being anisotropic ( $\gamma_2 \neq \gamma_3$ ), the eigenvectors of  $H_v$  are  $|\pm\frac{3}{2}\rangle$  for the heavy holes and  $|\pm\frac{1}{2}\rangle$  for the light holes but do not coincide with  $|\pm\frac{3}{2}\rangle$  and  $|\pm\frac{1}{2}\rangle$ : An eigenfunction  $|\bar{m}\rangle$  is a linear combination of wave

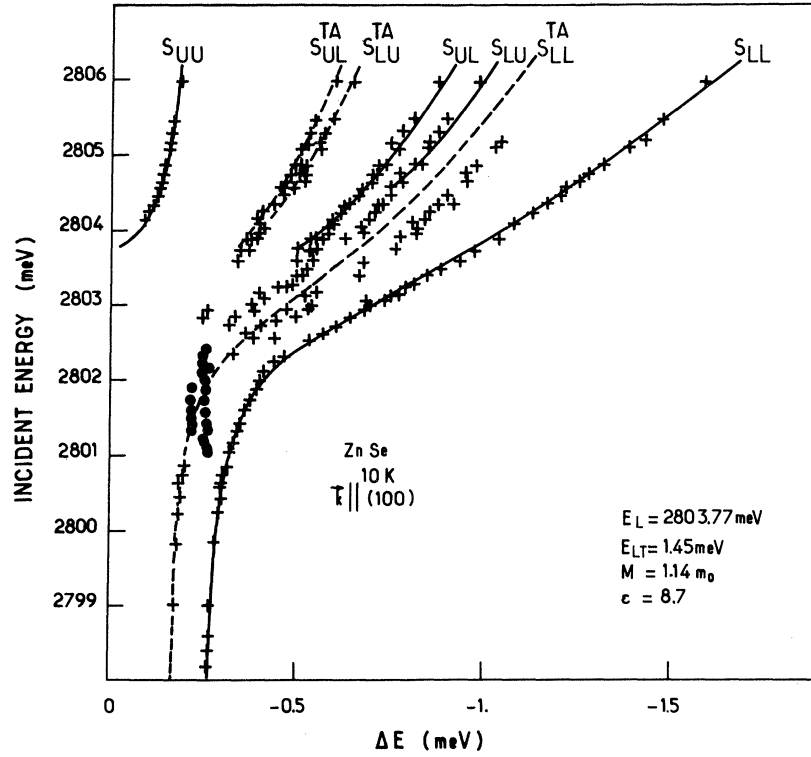


FIG. 7. Solid and dashed lines are calculated in a *two-branch polariton* model. Crosses (+) and solid circles (●) have the same meaning as in Fig. 4. A number of points, accounted for by the three-branch polariton model, should *not* exist in the two-branch model.

functions  $|m\rangle$ . For example,  $|\frac{3}{2}\rangle$  contains mainly the function  $|\frac{3}{2}\rangle$  and they coincide only in a high-symmetry direction [100] or [111] or in any direction if  $\gamma_2 = \gamma_3$ . Thus the calculations will be the same in the [100] and [111] directions but not in the [110] direction.

With the above notations the periodic part of the eigenfunctions of  $H_c + H_v$  is  $|\sigma\rangle \otimes |\vec{m}\rangle = |\sigma \vec{m}\rangle$ .

Now let us look at the eigenvalues. The eigen-

values of  $H_c$  are  $\hbar^2 k_e^2 / 2m_e$  (where  $2\pi\hbar$  is the Planck's constant,  $k_e$  and  $m_e$  are the wave vector and the effective mass of the conduction electron).

The eigenvalues of  $H_v$  are

$$(\hbar^2 k_h^2 / 2m_0) [\gamma_1 \pm f(\gamma_2, \gamma_3)]$$

where  $m_0$  is the free-electron mass,  $k_h$  the hole wave vector, and  $\gamma_1, \gamma_2,$  and  $\gamma_3$  are the Luttinger parameters).  $f(\gamma_2, \gamma_3)$  can be written as<sup>23</sup>

TABLE II. In the first column the Luttinger parameters  $\gamma_1, \gamma_2,$  and  $\gamma_3$  are obtained from the experimental determination of light and heavy exciton masses  $M_l$  and  $M_h$ . For the four other columns the masses  $M_l$  and  $M_h$  are deduced from the Luttinger parameters. All the calculations are done using Eqs. (66) and (67) of Ref. 1. The conduction electron mass is  $0.16m_0$  [after J. L. Merz, H. Kukimoto, K. Nassau, and J. W. Shiener, Phys. Rev. B 6, 545 (1972)].

		Our experiment	Reference 18	Reference 19	Reference 20	Reference 21
[100]	$M_l$	$0.38 \pm 0.05$	0.41	0.42	0.37	0.39
	$M_h$	$1.11 \pm 0.10$	2.0	0.87	0.56	0.58
[110]	$M_l$	$0.37 \pm 0.05$	0.37	0.4	0.34	0.33
	$M_h$	$1.95 \pm 0.10$	4.25	1.0	0.66	0.79
	$\gamma_1$	4.30	3.71	3.13	4.32	4.3
	$\gamma_2$	1.14	1.24	0.694	0.662	0.59
	$\gamma_3$	1.84	1.67	0.902	1.13	1.34

$$f(\gamma_2, \gamma_3) = 2 \left( \gamma_2^2 + 3(\gamma_3^2 - \gamma_2^2) \frac{k_x^2 k_y^2 + k_y^2 k_z^2 + k_z^2 k_x^2}{k^4} \right)^{1/2}. \quad (11)$$

$f(\gamma_2, \gamma_3)$  is, respectively, equal to  $2\gamma_2$ ,  $2\gamma_3$ , and  $(\gamma_2^2 + 3\gamma_3^2)^{1/2}$  in [100], [111], and [110] directions. The eigenvalues of  $H_c + H_v$  are

$$E_{\pm}(\vec{k}_e, \vec{k}_h) = \frac{\hbar^2 k_e^2}{2m_e} + \frac{\hbar^2 k_h^2}{2m_0} [\gamma_1 \pm f(\gamma_2, \gamma_3)] \quad (12)$$

and the splittings are

$$E_+(\vec{k}_e, \vec{k}_h) - E_-(\vec{k}_e, \vec{k}_h) = \frac{\hbar^2 k_h^2}{2m_0} 2f(\gamma_2, \gamma_3). \quad (13)$$

Now from a simple effective-mass exciton theory, where there is only one hole band of effective mass  $m_0/\gamma_1$  we know that ( $K$  being the exciton wave vector)

$$\vec{k}_e = \frac{m_e}{m_e + m_0/\gamma_1} \vec{K}, \quad (14)$$

$$\vec{k}_h = \frac{m_0/\gamma_1}{m_e + m_0/\gamma_1} \vec{K} = \beta_h \vec{K}, \quad \vec{K} = \vec{k}_e + \vec{k}_h$$

and we obtain

$$E_+(\vec{k}_e, \vec{k}_h) - E_-(\vec{k}_e, \vec{k}_h) = \frac{\hbar^2 K^2}{2m_0} \beta_h^2 2f(\gamma_2, \gamma_3). \quad (15)$$

Indeed the only thing we need to calculate the polariton dispersion curve in following sections (III B, III C, and III D) is to suppose (i) the periodic part of the eigenfunctions of  $H_K$  are  $|\sigma\vec{m}\rangle$  and (ii) the eigenvalues of  $|\sigma \pm \frac{3}{2}\rangle$  and  $|\sigma \pm \frac{1}{2}\rangle$  can be written  $E_h = \hbar^2 K^2 / 2M_h$  and  $E_l = \hbar^2 K^2 / 2M_l$  ( $M_h > M_l$ ); i.e., we can define an effective mass for each eigenvalue:  $|\sigma \pm \frac{3}{2}\rangle$  and  $|\sigma \pm \frac{1}{2}\rangle$  are, respectively, the wave functions of heavy and light excitons. We need no further hypothesis.

Now let us return to the calculation of Ref. 1. We have just seen that the Hamiltonian given by Eq. (10) is useful to make simple symmetry considerations but, just as it is, it cannot be used to make an effective calculation of the energies. To handle the Hamiltonian  $H_K$ , Kane writes

$$H_K = H_c + H_{v1} - \frac{e^2}{\epsilon r} + H_{v23}, \quad (16)$$

where  $H_c + H_{v1} - e^2/\epsilon r$  is the usual effective-mass Hamiltonian of the excitons (where the effective hole mass is  $m_0/\gamma_1$ ) and where  $H_{v23}$ , which gives the anisotropic splitting between heavy and light holes, is treated as a perturbation. The energy of the 1s exciton states is given by Eq. (64) of Ref. 1:

$$E_{1s}(\vec{K}) = R_a + \frac{\hbar^2 K^2}{2} \left( \frac{1}{M_a} \pm \frac{1}{M_c} \right), \quad (17)$$

where  $R_a$  is the Rydberg energy.

The splitting between heavy and light excitons is then given by

$$E_{1+}(\vec{K}) - E_{1-}(\vec{K}) = \frac{\hbar^2 K^2}{2} \frac{2}{M_c}. \quad (18)$$

Eq. (67) of Ref. 1 gives  $1/M_c$  which can be written as

$$\frac{1}{M_c} = \frac{\beta_h^2}{m_0} f(\gamma_2, \gamma_3) \quad (19)$$

so that Eq. (18) gives the same result as Eq. (15) as expected.

The significance of the above calculations is clear: We can obtain eigenvectors and splittings between the eigenvalues easily. Of course calculation of the exciton energies as a function of the exact values from the Luttinger parameters requires the knowledge of  $1/M_a$  and therefore the calculations of Ref. 1 or 15. Conversely these calculations are needed to obtain the Luttinger parameters when the heavy and light exciton masses are known. Finally, let us note that  $(m_e + m_0/\gamma_1)$  can be notably different from  $M_a$ : i.e., that the deviation with respect to an oversimplified effective-mass theory is important and also that it is difficult to define an average mass for the hole (and for the exciton) when the valence band is degenerate.

In the following the quantization axis will always be taken parallel to the exciton wave vector.

## B. Exchange interaction

In Sec. III A as well as in Ref. 1, the exchange interaction between electron and hole has not been taken into account. The corresponding Hamiltonian can be divided into two parts: an anisotropic one which we neglect because there is no evidence for it in ZnSe and an isotropic one which is given below. (To be exact the isotropic part of the exchange interaction includes terms depending on the modulus of wave vector but we do not take into account these terms and from now on we call exchange interaction the part of the exchange interaction which does not depend at all on the wave vector.)

Let us first give some precisions on the exciton wave functions. Until now we have used the  $|\sigma\vec{m}\rangle$  and  $|\sigma m\rangle$  basis. However, the exchange interaction can be expressed simply in the  $|JM\rangle$  basis which is a known linear combination of the  $|\sigma m\rangle$  functions. The  $|JM\rangle$  basis is divided into a quintuplet state  $|2M\rangle$  and a triplet state  $|1M\rangle$ . It is well known<sup>24</sup> that the  $|2M\rangle$  functions are not coupled to light, the  $|10\rangle$  functions are longitudinal states and the  $|1\pm 1\rangle$  functions are the two transverse states which are the only ones to be coupled to light. For the polariton effect the

wave functions of interest are the wave functions which are mixed with these transverse states.

The problem is now to diagonalize the sum of two Hamiltonians: the kinetic-energy Hamiltonian  $H_K$  (diagonal in the  $|\sigma\bar{m}\rangle$  basis) and the exchange interaction (diagonal in the  $|JM\rangle$  basis). The short-range part of the exchange interaction splits the eightfold-degenerate level  $|JM\rangle$  into two degenerate levels: the quintuplet one  $|2M\rangle$  and the triplet one  $|1M\rangle$ , the difference  $\Delta$  between these two levels being the so-called exchange energy. The long-range part of the exchange interaction splits the triplet level into two levels: the longitudinal one  $|10\rangle$  and the twofold-degenerate transverse one  $|1\pm 1\rangle$ . The splitting  $E_{LT}$  between these two levels is the so-called longitudinal-transverse splitting hereafter denoted LTS. The splitting  $\delta$  between the quintuplet state and the transverse triplet state will be called quintuplet-transverse splitting hereafter denoted QTS. In other words,  $E_{LT} = E(10) - E(1\pm 1)$ ,  $\delta = E(1\pm 1) - E(2M)$ , where  $E(JM)$  is the energy of the  $|JM\rangle$  state at  $K=0$ . It is worth noting that optical experiments permit us to measure the LTS and the QTS but not directly the exchange energy.

In the ideal case where (i) the background dielectric constant is equal to one and (ii) excitons are of the Frenkel type, the long-range part of the exchange interaction preserves the center of gravity of the triplet state; the longitudinal-state energy is increased by  $\frac{2}{3}E_{LT}$  and the transverse-state energy is decreased by  $\frac{1}{3}E_{LT}$  so that the QTS  $\delta$  is equal to  $\delta = \Delta - \frac{1}{3}E_{LT}$ . This relation has been used in some papers dealing with semiconductors.<sup>12,25</sup> However, in this last case neither of the conditions (i) and (ii) is satisfied so that the above relation between  $\delta$ ,  $\Delta$ , and  $E_{LT}$  is no longer satisfied. The center of gravity of the triplet level is not conserved by the long-range part of the exchange interaction and very likely is merely equal to the exchange energy  $\Delta$ .<sup>26</sup> In any case the attainable experimental parameters  $E_{LT}$  and  $\delta$  are the useful parameters in polariton effect.

The exchange interaction Hamiltonian can be written as  $H_{\text{exch}} = H_{\text{SR}} + H_{\text{LR}}$ , where  $H_{\text{SR}}$  and  $H_{\text{LR}}$  correspond, respectively, to the short-range part ( $\Delta$ ) and to the long-range part ( $E_{LT}$ ) of the exchange interaction. However, we prefer to write it in a more convenient form, displaying the quantities  $\delta$  and  $E_{LT}$  instead of  $\Delta$  and  $E_{LT}$  as follows:

$$H_{\text{exch}} = H_1 + H_2, \quad (20)$$

where

$$H_1 = \delta \delta_{J_1}, \quad (21)$$

$$H_2 = E_{LT} \delta_{J_1} \delta_{M_0}. \quad (22)$$

$\delta_{J_1}$  and  $\delta_{M_0}$  are Kronecker symbols.

In this form  $H_{\text{exch}}$  is valid whatever may be the relation between  $\delta$ ,  $\Delta$ , and  $E_{LT}$ . In Eqs. (20), (21), and (22) the wave-vector direction (and therefore the quantization axis which is parallel to it) is arbitrary, i.e.,  $H_{\text{exch}}$  is isotropic.

### C. Exciton dispersion curve

Now the problem is to calculate the eigenfunctions and the eigenvalues of the Hamiltonian

$$H_K + H_{\text{exch}}.$$

We know that the eigenfunctions of these two Hamiltonians are, respectively,  $|\sigma\bar{m}\rangle$  and  $|JM\rangle$ . Let us look at the  $|\sigma\bar{m}\rangle$  functions. In  $H_K$  the only off-diagonal elements proceed from  $H_{v23}$  so that we must diagonalize  $H_{v23}$ . We will study more particularly the case of the [110] direction; the case of the [100] direction has been reported in Ref. 12.

In the [110] direction the useful part of  $H_{v23}$  can be written in the  $|m\rangle$  basis<sup>23</sup> as

$$\begin{pmatrix} |\frac{3}{2}\rangle & |\frac{1}{2}\rangle & |-\frac{1}{2}\rangle & |-\frac{3}{2}\rangle \\ -\frac{1}{2}\gamma_2 - \frac{3}{2}\gamma_3 & 0 & \frac{\sqrt{3}}{2}(\gamma_2 - \gamma_3) & 0 \\ 0 & \frac{1}{2}\gamma_2 + \frac{3}{2}\gamma_3 & 0 & \frac{\sqrt{3}}{2}(\gamma_2 - \gamma_3) \\ \frac{\sqrt{3}}{2}(\gamma_2 - \gamma_3) & 0 & \frac{1}{2}\gamma_2 + \frac{3}{2}\gamma_3 & 0 \\ 0 & \frac{\sqrt{3}}{2}(\gamma_2 - \gamma_3) & 0 & -\frac{1}{2}\gamma_2 - \frac{3}{2}\gamma_3 \end{pmatrix}. \quad (23)$$

The eigenfunctions of this Hamiltonian are

$$\begin{aligned} |\frac{3}{2}\rangle &= a |\frac{3}{2}\rangle + b |-\frac{1}{2}\rangle, & |\frac{1}{2}\rangle &= a |\frac{1}{2}\rangle - b |-\frac{3}{2}\rangle, \\ |-\frac{3}{2}\rangle &= a |-\frac{3}{2}\rangle + b |\frac{1}{2}\rangle, & |-\frac{1}{2}\rangle &= a |-\frac{1}{2}\rangle - b |\frac{3}{2}\rangle. \end{aligned} \quad (24)$$

$a$  and  $b$  can be written explicitly if needed,  $a^2 + b^2 = 1$ , and usually  $a \gg b$  ( $a$  and  $b$  can be taken as real and positive).  $a/b$  depends on  $(\gamma_3 - \gamma_2)/\gamma_2$ :  $a$  and  $b$  are given for different values of this ratio in Table III. Of course it is a straightforward matter to obtain  $|m\rangle$  functions versus  $|\bar{m}\rangle$  functions.

To write the matrix  $H_K + H_{\text{exch}}$  in the  $|JM\rangle$  basis we have expressed the  $|JM\rangle$  functions in the  $|\sigma\bar{m}\rangle$  basis; see the Appendix. We now have the following:

$$\begin{aligned} \langle 10 | (H_K + H_{\text{exch}}) | 10 \rangle &= a^2 E_l + b^2 E_h + \delta + E_{LT}, \\ \langle 20 | (H_K + H_{\text{exch}}) | 20 \rangle &= a^2 E_l + b^2 E_h, \\ \langle 2 \pm 2 | (H_K + H_{\text{exch}}) | 2 \pm 2 \rangle &= a^2 E_h + b^2 E_l. \end{aligned} \quad (25)$$



TABLE III. Mixing of the  $|\sigma m\rangle$  functions for  $\vec{k}||[110]$  for different values of  $(\gamma_3 - \gamma_2)/\gamma_2$ .  $\gamma_2$  and  $\gamma_3$  are Luttinger parameters and  $a$  and  $b$  are defined in the text [see Eq. (24)].

$\frac{\gamma_3 - \gamma_2}{\gamma_2}$	$a$ ( $a^2$ )	$b$ ( $b^2$ )
0	1 (1)	0 (0)
0.5	0.997 (0.994)	0.078 (0.006)
1.0	0.993 (0.986)	0.121 (0.014)
1.5	0.989 (0.978)	0.145 (0.022)

[The origin of the energy scale is such that  $E(2M) = 0$ ]. All other matrix elements with  $|10\rangle$ ,  $|20\rangle$ ,  $|22\rangle$ , and  $|2-2\rangle$  are equal to zero. We see that, contrary to the case where the wave vectors are parallel to  $[100]$  or  $[111]$  (where  $a=1$ ,  $b=0$ ), the wave functions  $|10\rangle$ ,  $|20\rangle$ , and  $|2\pm 2\rangle$  do not correspond to pure light or heavy excitons. However, from Table III we see that the mixing is very weak.

The coupling with light is given by the matrix given in Table IV. The eigenvalues  $\lambda$  are solutions of

$$\lambda^2 - (E_l + E_h + \delta)\lambda + E_l E_h + (E_l + E_h)\delta/4 + (a^2 E_l + b^2 E_h)\delta/2 \pm (\sqrt{3}/2)[ab(E_l - E_h)\delta] = 0. \quad (26)$$

TABLE IV. Matrix giving the mixing of the wave functions  $|1\pm 1\rangle$  coupled to light to other functions inside the space  $|JM\rangle$ ,  $J=1$  or  $2$  in the  $[110]$  direction (without taking into account the linear  $k$  term).  $E_l$  and  $E_h$  are, respectively, the kinetic energy of light and heavy excitons.  $a$  and  $b$  are defined by Eq. (24) of this paper. The quantization axis is parallel to  $[110]$ . The *exact* eigenvalues of this matrix are given by Eq. (26).

$ 11\rangle$	$ 21\rangle$	$ 1-1\rangle$	$ 2-1\rangle$
$\frac{a^2 + 3b^2}{4} E_l + \frac{3a^2 + b^2}{4} E_h + \delta$	$-\frac{\sqrt{3}(a^2 - b^2)}{4} (E_l - E_h)$	$-\frac{\sqrt{3} ab}{2} (E_l - E_h)$	$-\frac{ab}{2} (E_l - E_h)$
$-\frac{\sqrt{3}(a^2 - b^2)}{4} (E_l - E_h)$	$\frac{3a^2 + b^2}{4} E_l + \frac{a^2 + 3b^2}{4} E_h$	$\frac{ab}{2} (E_l - E_h)$	$-\frac{\sqrt{3} ab}{2} (E_l - E_h)$
$-\frac{\sqrt{3} ab}{2} (E_l - E_h)$	$\frac{ab}{2} (E_l - E_h)$	$\frac{a^2 + 3b^2}{4} E_l + \frac{3a^2 + b^2}{4} E_h + \delta$	$\frac{\sqrt{3}(a^2 - b^2)}{4} (E_l - E_h)$
$-\frac{ab}{2} (E_l - E_h)$	$-\frac{\sqrt{3} ab}{2} (E_l - E_h)$	$\frac{\sqrt{3}(a^2 - b^2)}{4} (E_l - E_h)$	$\frac{3a^2 + b^2}{4} E_l + \frac{a^2 + 3b^2}{4} E_h$

In the isotropic case ( $\gamma_2 = \gamma_3$ ,  $b=0$ ) there are only two two-by-two matrices and we find again the solutions of Ref. 12 valid in the  $[100]$  and  $[111]$  directions. In the general case Eq. (26) leads to a four-branch exciton dispersion curve coupled to light and therefore a five-branch polariton dispersion curve in the  $[110]$  direction. The four-branch exciton dispersion curve exists if these three conditions are satisfied: (i)  $\gamma_2$  or  $\gamma_3 \neq 0$  which means that there are two kinds of excitons ( $E_l \neq E_h$ ), (ii) the  $|\bar{m}\rangle$  functions are not identical to  $|m\rangle$  functions ( $ab \neq 0$ ), and (iii) the QTS  $\delta$  is not equal to zero.

Let us calculate an order of magnitude of these further splittings in ZnSe. Let us take  $\delta \sim 0.1$  meV,  $K \sim 10^6$  cm $^{-1}$ ; we find  $E_l - E_h \sim 0.6$  meV but the new splitting for each (heavy and light) exciton branch is only of the order of  $0.02$  meV  $\ll 0.6$  meV.

This splitting is very small and it is not surprising that we have not observed it in ZnSe: A quasi-isotropic model is quite enough to explain our results. As usual in a first-order perturbation theory it is enough to modify the eigenvalues ( $E_l$  and  $E_h$  and therefore  $M_l$  and  $M_h$ ) following the direction of wave vectors but not the eigenvectors ( $a^2 \sim 1$ ,  $b^2 \ll 1$ ) and to suppose that eigenstates are given by the two-by-two matrix obtained if  $a=1$ ,  $b=0$ . More precisely we say that a model is quasi-isotropic if only a two-by-two matrix is considered and if the dependence on the wave-vector direction is taken into account only through the exciton masses and not through the wave functions.

Now let us make some remarks on the number of polariton branches. Only the eigenvalues of

$H_{\text{exch}}$  are isotropic, unlike those of  $H_K$ ,  $E_l$ , and  $E_h$  which depend on the wave-vector direction. Thus for an unspecified wave-vector direction eight different eigenvalues can be found, because the dimension of  $\Gamma_6 \times \Gamma_8$  is equal to eight. For example, in the [110] direction whose symmetry is not very low we have found four branches coupled to the light and therefore a five-branch polariton. We wish to emphasize that this is obtained without the linear  $k$  term, with which a four-branch exciton can be obtained in the [110] direction.

#### D. Linear $k$ term

In the [110] direction the linear  $k$  term splits the valence band in four sublevels, but this has not been observed in our experiments and we do not think that it is useful to take this term into account. However, in the [100] direction the splitting due to this term leads to two branches and cannot be set aside at first view. Using the method of Hopfield and Mahan,<sup>27</sup> the Hamiltonian which takes into account the linear  $k$  term in the [100] direction is written

$$\begin{pmatrix} |11\rangle & |21\rangle & |1-1\rangle & |2-1\rangle \\ \frac{E_l + 3E_h}{4} + \delta & -\frac{\sqrt{3}}{4}(E_l - E_h) & 0 & CK \\ -\frac{\sqrt{3}}{4}(E_l - E_h) & \frac{3E_l + E_h}{4} & CK & 0 \\ 0 & CK & \frac{E_l + 3E_h}{4} + \delta & \frac{\sqrt{3}}{4}(E_l - E_h) \\ CK & 0 & \frac{\sqrt{3}}{4}(E_l - E_h) & \frac{3E_l + E_h}{4} \end{pmatrix}. \quad (27)$$

The constant  $C$  used here is equal to that of Eq. 57 of (Ref. 28) multiplied by  $m_0/(\gamma_1 m_e + m_0)$ . If  $C=0$ , we find again the solutions of Ref. 12. The two twofold-degenerate eigenvalues are

$$\lambda_{\pm} = \frac{1}{2}\{E_l + E_h + \delta \pm [(E_l + E_h + \delta)^2 - 4E_l E_h + 4C^2 K^2]^{1/2}\} \quad (28)$$

The four eigenvectors have the form

$$\alpha_{i\pm} |11\rangle + \alpha'_{i\pm} |1-1\rangle + \alpha''_{i\pm} |21\rangle + \alpha'''_{i\pm} |2-1\rangle, \quad (29)$$

where the index + or - corresponds to the eigenvalues  $\lambda_+$  or  $\lambda_-$ . For each eigenvalue there are two eigenvectors:  $i=1, 2$ . The normalization gives

$$(\alpha_{i\pm})^2 + (\alpha'_{i\pm})^2 + (\alpha''_{i\pm})^2 + (\alpha'''_{i\pm})^2 = 1, \quad (30)$$

and the coupling to light is given by

$$4\pi\beta_{\pm} = 4\pi\beta_0 [(\alpha_{1\pm})^2 + (\alpha'_{1\pm})^2] = 4\pi\beta_0 [(\alpha_{2\pm})^2 + (\alpha'_{2\pm})^2], \quad (31)$$

where  $4\pi\beta_0$  is the oscillator strength which is related to the LTS  $E_{LT}$  at  $K=0$ .

The polariton curve is given by

$$\frac{\hbar^2 c^2 K^2}{E^2} = \epsilon + \frac{4\pi\beta_+}{1 - (E/\lambda_+)^2} + \frac{4\pi\beta_-}{1 - (E/\lambda_-)^2}. \quad (32)$$

A discussion on the importance of the linear  $k$  term in the polariton dispersion curve is given in the following section.

#### IV. DISCUSSION

Figure 4 shows that the linear  $k$  term improves only slightly the agreement between the theoretical curve and the experimental points in the [100] direction. Though the curve is not very sensitive to the value of  $C$ , the best fit is obtained for  $C = 3 \times 10^{-10}$  eV cm which compares favorably to  $C = 5 \times 10^{-10}$  eV cm obtained in CdTe.<sup>25</sup> The values of the four parameters  $E_{LT}$ ,  $\delta$ ,  $M_l$ , and  $M_h$  are given in Table II. From Table II and Fig. 4 it is seen that in the [100] direction the linear  $k$  term does not change the values of  $E_{LT}$  and  $\delta$  while the values of heavy and light exciton masses are only slightly different. This last point shows that we can be confident in the values of these four parameters but the value of  $C$  quoted here is not very precise. We wish to point out that we have only supposed that the exchange interaction is isotropic and that the exciton dispersion can be accounted for by two effective masses (the wave functions needed for the calculation of the polariton dispersion curve being developed inside a  $\Gamma_6 \times \Gamma_8$  space). In the [110] direction it is still less realistic to take into account the linear  $k$  term because there is no experimental evidence for further splittings induced by this term.

From the values of the exciton masses in the [100] and [110] directions we have calculated the Luttinger parameters using Eqs. (66) and (67) of Ref. 1. The values are quoted in Table II. However, Luttinger parameters are very sensitive to

the exact values of the exciton masses.<sup>1,15</sup> As a matter of fact it seems to us that the values quoted in the literature must be taken with caution in semiconductors with a degenerate valence band.<sup>29</sup>

Anyway, the fits of Figs. 4 and 5 show that the Kane model is widely sufficient to account for the details of experimental results.<sup>30</sup> Now it is known that this model can be improved (a full discussion is given in Ref. 15). So we must wonder about the physical reason why the simple model used in this paper works so well in ZnSe. In our opinion it is because the QTS  $\delta$  is weak and thus the mixing of the wave functions of heavy and light excitons can be neglected even for  $k$  different from zero and therefore the oscillator strength of each branch is nearly constant (i.e., independent of the magnitude of  $k$ ). In this case the details of the wave function do not have much importance in fitting the experimental curves if the masses of heavy and light excitons are taken as unknown parameters. At the same time in this case, the model which is, strictly speaking, valid only in the [100] direction becomes valid for all directions, the exciton masses being parameters which depend on the  $k$  direction: We obtain the quasi-isotropic model described in Sec. III B.

We can note that,  $\delta$  being negligible, the oscillator strength of the heavy exciton branch is equal to  $\frac{3}{4}(4\pi\beta_0)$  and gives rise to an apparent LTS for this branch  $E_{LT} = \frac{3}{4}(1.45 \text{ meV}) = 1.1 \text{ meV}$ , which is very near the values usually quoted in literature. Although we have no definitive explanation of this agreement we think that this conderation has to be taken into account for comparison with other experiments.

If the QTS is not weak, the situation can become quite different: The use of the matrix of Table IV is needed. Then, it is not sure that the model of Ref. 1 is sufficient, because in such a case the very details of the wave function would be needed and the method of Ref. 15 would become necessary: The calculation including polariton effect would become much more difficult.

In conclusion, we wish to make a remark on the possible mixing between longitudinal and transverse excitons in an unspecified wave-vector direction.<sup>24</sup> In our calculation in the [110] direction the  $|10\rangle$  state is purely longitudinal, i.e.,  $|10\rangle$  is an eigenvector of  $H_K + H_{\text{exch}}$ . This occurs only when the linear  $k$  term is neglected. If this term is taken into account, the longitudinal and transverse exciton are mixed.<sup>11</sup>

## V. CONCLUSION

We have shown that the notion of heavy and light excitons in degenerate valence-band semiconduc-

tors is very realistic. From an experimental point of view the useful parameters are the longitudinal-transverse splitting, the quintuplet-transverse (triplet) splitting, and the two masses of heavy and light excitons, these two last parameters depending on the direction of the wave vectors. In ZnSe the values of these parameters are not very sensitive to the theory used (for example, taking into account or not the linear  $k$  term).

Taking into account the isotropic part of the exchange energy we have shown that theoretically the number of branches of the dispersion curve of heavy and light excitons (and therefore the number of branches of the polariton dispersion curve) depends on the wave-vector direction. For example, the number of branches is equal to two in the [100] direction and to four in the [110] direction leading to a five-branch polariton dispersion curve in this last case.

However, if the QTS can be neglected (i.e., if the QTS is much weaker than the LTS which is the case in ZnSe), a quasi-isotropic model is enough to account for the experimental results. In any case the determination of the exchange energy and Luttinger parameters can only be done in the framework of a model but cannot be directly deduced from the resonant Brillouin scattering experiment.

## ACKNOWLEDGMENTS

We wish to thank C. Benoit a' la Guillaume, R. Bonneville, C. Hermann, B. Hönerlage, G. Lampel, D. Paquet, and C. Weisbuch for valuable discussions and U. Rössler for communication of results prior to publication. We are very indebted to P. Henoc who succeeded in obtaining oriented monocrystalline faces from polycrystalline samples and to P. Blanconnier who has grown very-high-purity samples. The numerical computations have been performed by Mrs. F. Bonnouvrier.

## APPENDIX

We give here the expression the  $|JM\rangle$  functions in  $|\sigma\tilde{m}\rangle$  basis in [110] direction. The quantization axis is parallel to [110]. We have the following:

$$\begin{aligned} |22\rangle &= a \left| \uparrow \frac{3}{2} \right\rangle - b \left| \uparrow - \frac{1}{2} \right\rangle, \\ |21\rangle &= \frac{1}{2} [a ( \left| \uparrow \frac{3}{2} \right\rangle + \sqrt{3} \left| \uparrow \frac{1}{2} \right\rangle ) - b ( \left| \uparrow - \frac{1}{2} \right\rangle - \sqrt{3} \left| \uparrow - \frac{3}{2} \right\rangle )], \\ |20\rangle &= \frac{1}{\sqrt{2}} [a ( \left| \uparrow \frac{1}{2} \right\rangle + \left| \uparrow - \frac{1}{2} \right\rangle ) + b ( \left| \uparrow - \frac{3}{2} \right\rangle + \left| \uparrow \frac{3}{2} \right\rangle )], \\ |2-1\rangle &= \frac{1}{2} [a (\sqrt{3} \left| \uparrow - \frac{1}{2} \right\rangle + \left| \uparrow - \frac{3}{2} \right\rangle) - b ( \left| \uparrow \frac{1}{2} \right\rangle - \sqrt{3} \left| \uparrow \frac{3}{2} \right\rangle )], \\ |2-2\rangle &= a \left| \uparrow - \frac{3}{2} \right\rangle - b \left| \uparrow \frac{1}{2} \right\rangle, \\ |11\rangle &= \frac{1}{2} [a (\sqrt{3} \left| \uparrow \frac{3}{2} \right\rangle - \left| \uparrow \frac{1}{2} \right\rangle) - b (\sqrt{3} \left| \uparrow - \frac{1}{2} \right\rangle + \left| \uparrow - \frac{3}{2} \right\rangle)], \end{aligned}$$

$$|10\rangle = \frac{1}{\sqrt{2}} [a(|\uparrow\frac{1}{2}\rangle - |\uparrow - \frac{1}{2}\rangle) + b(|\uparrow - \frac{3}{2}\rangle - |\uparrow\frac{3}{2}\rangle)],$$

$$|1-1\rangle = \frac{1}{2} [a(|\uparrow - \frac{1}{2}\rangle - \sqrt{3} |\uparrow - \frac{3}{2}\rangle) + b(\sqrt{3} |\uparrow\frac{1}{2}\rangle + |\uparrow\frac{3}{2}\rangle)].$$

The  $|\bar{m}\rangle$  functions are given by Eq. (24). If  $\gamma_2 = \gamma_3$ ,  $a = 1$ , and  $b = 0$ , and we find again the standard definition of the  $|JM\rangle$  functions where  $|\bar{m}\rangle = |m\rangle$ .

\*Laboratoire associé au Centre National de la Recherche Scientifique.

<sup>1</sup>E. O. Kane, Phys. Rev. B **11**, 3850 (1975).

<sup>2</sup>G. Dresselhaus, J. Phys. Chem. Solids **1**, 14 (1956).

<sup>3</sup>A. Frova, G. A. Thomas, R. E. Millev, and E. O. Kane, Phys. Rev. Lett. **34**, 1572 (1975).

<sup>4</sup>S. I. Pekar, Zh. Eksp. Teor. Fiz. **33**, 1022 (1957) [Sov. Phys.—JETP **6**, 785 (1958)].

<sup>5</sup>J. J. Hopfield, Phys. Rev. **112**, 1555 (1958).

<sup>6</sup>W. Brenig, R. Zeiher, and J. L. Birman, Phys. Rev. B **6**, 4617 (1972).

<sup>7</sup>R. G. Ulbrich and C. Weisbuch, Phys. Rev. Lett. **38**, 865 (1977).

<sup>8</sup>G. Winterling and E. Koteles, Solid State Commun. **23**, 95 (1977).

<sup>9</sup>C. Hermann and P. Y. Yu, Solid State Commun. **28**, 313 (1978); C. Hermann and P. Y. Yu, Phys. Rev. B **21**, 3675 (1980).

<sup>10</sup>B. Hönerlage, A. Bivas, and Vu Duy Phach, Phys. Rev. Lett. **41**, 49 (1978).

<sup>11</sup>B. Hönerlage, U. Rössler, Vu Duy Phach, A. Bivas, and J. G. Grun, Phys. Rev. B **22**, 797 (1980).

<sup>12</sup>G. Fishman, Solid State Commun. **27**, 1097 (1978).

<sup>13</sup>G. Fishman, J. Lumin. **18**, 289 (1979).

<sup>14</sup>B. Sermage and G. Fishman, Phys. Rev. Lett. **43**, 1043 (1979).

<sup>15</sup>M. Altarelli and N. O. Lipari, Phys. Rev. B **15**, 4898 (1977).

<sup>16</sup>G. Dresselhaus, Phys. Rev. **100**, 580 (1955).

<sup>17</sup>B. H. Lee, J. Appl. Phys. **41**, 2984 (1970).

<sup>18</sup>P. Lawaetz, Phys. Rev. B **4**, 3460 (1971).

<sup>19</sup>M. Sondergeld, Phys. Status Solidi B **81**, 253 (1977).

<sup>20</sup>S. Feierabend and H. G. Weber, Solid State Commun. **26**, 191 (1978).

<sup>21</sup>H. Venghaus, Phys. Rev. B **19**, 3071 (1979).

<sup>22</sup>We have performed resonant Brillouin scattering experiments (RBS) in [111] direction. However, for unclear reasons (strain in the sample?) we have not been able to ascribe all the lines of the RBS spectra to a definite origin. From the identified lines we have measured in [111] direction  $M_R = 1.96 \pm 0.10$  and  $M_I = 0.41 \pm 0.05$ .

<sup>23</sup>J. M. Luttinger, Phys. Rev. **102**, 1030 (1956).

<sup>24</sup>R. S. Knox, *Theory of Excitons*, Suppl. 5 of *Solid State Physics*, edited by F. Seitz and D. Turnbull (Academic, New York, 1964).

<sup>25</sup>W. Dreybrodt, K. Cho, S. Suga, F. Willmann, and Y. Niji, Phys. Rev. B **21**, 4692 (1980).

<sup>26</sup>See a discussion in R. Bonneville and G. Fishman, Phys. Rev. B **22**, 2008 (1980). In Refs. 12–14 the exchange energy  $\Delta$  was supposed to be equal to  $\Delta = \delta + \frac{1}{3}E_{LT}$ . Here we take  $\Delta = \delta$ . The (wrong) value  $\Delta = 2.1$  meV of Ref. 14 must be indeed compared to  $\delta + \frac{1}{3}E_{LT} \sim 0.5$  meV and not to  $\Delta \sim \delta \sim 0$  meV which is given in this paper.

<sup>27</sup>G. D. Mahan and J. J. Hopfield, Phys. Rev. **135**, A428 (1964).

<sup>28</sup>E. O. Kane, *Physics of III-V Compounds* (Academic, New York, 1966), Vol. I, p. 75.

<sup>29</sup>See a discussion in C. Uihlein and S. Feierabend, Phys. Status Solidi B **94**, 153 (1979).

<sup>30</sup>As in previous cases (see, for example, Ref. 7) the agreement between experimental points and theoretical curves is better for intrabranched than for interbranch transitions. This results from the fact that the parameters have been obtained by fitting only the intrabranched transitions, the interbranch ones being calculated in a second step.